

Exosomal-miR-32-5p directly targets FOXN2 to regulate the proliferation, migration and apoptosis of uterine corpus endometrial carcinoma via the PI3K/AKT/BCL-2 pathway

XIN CHEN^{1*}, HUIHUI LI^{2*}, XIANG CHENG¹, YIRONG CAI³ and GUANGYI GUO³

¹Department of Oncology, Renmin Hospital of Wuhan University, Wuhan, Hubei 430060, P.R. China; ²Department of Healthcare Center, Union Hospital, Tongji Medical College, Huazhong University of Science and Technology, Wuhan, Hubei 430022, P.R. China;

³Department of Oncology, Traditional Chinese Medicine Hospital of Xishui County, Huanggang, Hubei 438000, P.R. China

Received June 23, 2024; Accepted August 14, 2025

DOI: 10.3892/ol.2026.15574

Abstract. The transfer of microRNAs (miRNAs) between cells through exosomes is crucial in controlling the expression of various target genes in the recipient cells, giving exosomal miRNAs the capability to control the advancement of tumors. The present study aimed to explore the function of exosomal miR-32-5p in the *in vitro* progression of uterine corpus endometrial carcinoma (UCEC). Bioinformatics analyses were applied to identify potential miRNAs in UCEC. Forkhead Box N2 (FOXN2) was subsequently predicted as a putative target gene of miR-32-5p, followed by examination through a luciferase reporter assay. Exosomes derived from UCEC cells or plasma samples of patients with UCEC were examined. The biological functions of miR-32-5p or exosomal miR-32-5p were determined by cell phenotype experiments. Protein and mRNA expression in UCEC cells were assessed through western blotting and quantitative reverse transcription-PCR, respectively. miR-32-5p demonstrated the most significant effects on survival probability, therefore it was selected for further investigation in the present study. miR-32-5p was observed to be enriched in plasma exosomes and significantly upregulated in cancer tissues, as well as in cancer plasma exosomes. The present findings demonstrated that exosomal-miR-32-5p could induce the proliferation, migration

and suppress apoptosis of UCEC cells through regulation of the FOXN2/PI3K/AKT/Bcl-2 pathway, thus exhibiting potential as therapeutic target against UCEC.

Introduction

Uterine corpus endometrial carcinoma (UCEC) is a prevalent form of cancer in women, and its incidence is rapidly increasing (estimated annual percentage change, 0.69% per year) while its mortality is decreasing (estimated annual percentage change, 0.85% per year) worldwide in recent years (1). UCEC can be broadly classified into two primary subtypes: Type I, which is hormone-driven and generally associated with a favorable prognosis; and type II, which is hormone-independent and typically characterized by a poorer prognosis (2). In China, the majority of newly diagnosed UCEC cases (80-90%) fall under type I classification (3). A notable proportion of UCEC type I cases are detected at an early stage, leading to favorable outcomes with standard surgical intervention and subsequent chemotherapy; the 5-year relative survival rate for such patients is ~80% (4,5). However, certain patients experiencing recurrent UCEC may not achieve satisfactory therapeutic responses from existing treatment modalities. The unfavorable outcome of these individuals is primarily attributed to the malignant growth and distant metastasis (6,7). Therefore, comprehending the underlying mechanisms governing malignant behaviors in UCEC is of importance.

The interaction between cells serves a significant role in influencing the progression of tumors, and several studies have demonstrated its direct impact on tumor metastasis (8,9). Communication among cells within the microenvironment can be facilitated through extracellular exosomes (10). Extracellular membranous vesicles known as exosomes, ranging from 30 to 150 nm in size, consist of proteins, lipids, DNAs and various forms of RNAs (11). Following fusion with the cytoplasmic membrane, exosomes are released into the extracellular space by most cell types (12). Subsequently, recipient cells internalize these exosomes for modulation purposes. Previous studies suggest that the intercellular transfer of microRNA (miRNA) via exosomes serves a pivotal role in modulating the expression levels of multiple target

Correspondence to: Dr Xin Chen, Department of Oncology, Renmin Hospital of Wuhan University, 99 Zhangzhidong Road, Wuhan, Hubei 430060, P.R. China
E-mail: whdxchenxin@163.com

*Contributed equally

Abbreviations: miRNA, microRNA; mRNA, messenger RNA; UCEC, uterine corpus endometrial carcinoma; TCGA, The Cancer Genome Atlas; DE, differentially expressed; EdU, 5-ethynyl-2'-deoxyuridine; WT, wild-type; MUT, mutant

Key words: exosome, miR-32-5p, uterine corpus endometrial carcinoma, proliferation, migration, apoptosis

genes within recipient cells, thereby endowing exosomes with the ability to regulate tumor cell proliferation, migration and invasion (13,14). Recently, numerous exosomal miRNAs, such as exosomal miR-27a-5p (15) and miR-499a-5p (16), have been reported to mediate the development of UCEC. miR-32-5p has been implicated as an oncogenic factor in pancreatic (17), colorectal (18) and gynecological cancer, such as ovarian cancer (19). However, its role in UCEC progression remains elusive. Furthermore, it was recently demonstrated that serum exosomal miR-32-5p holds potential as a diagnostic biomarker for coronary artery disease (20). Therefore, the impact of exosomal miR-32-5p on the progression of UCEC and its underlying mechanism has gained notable interest in current research.

The present study aimed to investigate the expression of miR-32-5p in UCEC, and perform preliminary investigations into the role and mechanism of exosomal miR-32-5p during the progression of UCEC.

Materials and methods

Data acquisition. miRNA expression data in UCEC were downloaded from The Cancer Genome Atlas (TCGA) database (<https://portal.gdc.cancer.gov/>). A cohort comprising 578 samples were analyzed, with 33 categorized as normal and 545 as UCEC tumor samples. Additionally, 49 DE-miRNAs previously identified by Zhou *et al* (21) from the comparison of 56 plasma samples from patients with endometrial cancer and healthy controls were analyzed in the present study.

Screening of differentially expressed (DE) miRNAs. The Limma package (version 3.52.0; Bioconductor) was employed for the analysis of DE-miRNAs between UCEC and normal samples. miRNAs with a false discovery rate ≤ 0.05 , \log_2 fold change ≥ 1.2 and P-value < 0.01 were considered to be statistically significant. The 49 DE-miRNAs identified from analysis by Zhou *et al* (21) were included in the present study analysis.

Patient samples. From October 2023 to April 2024, a total of 9 patients (age, 44-72 years; mean age, 57.56 ± 8.93 years) diagnosed with UCEC via pathological examination were enrolled in Renmin Hospital of Wuhan University (Wuhan, China). Inclusion criteria: Patients had been admitted to the hospital for the first time and did not receive any malignant tumor treatments, such as chemotherapy or radiotherapy before surgery; postoperative tissues were diagnosed by pathologists as UCEC with parallel International Federation of Gynecology and Obstetrics (FIGO) staging; patients were aware of and agreed to the present study process; and patient clinical data and follow-up data were complete and available. Exclusion criteria: Patients with other malignant tumors; patients with immune system diseases or infectious diseases; and patients with severe impairment of the heart, liver, kidney and other organ functions. According to the FIGO staging system (22), the tumor stages of the included patients were as follows: Stage I, 1; stage III, 1; and stage IV, 7 cases. A total of 9 sex and age-matched healthy individuals were recruited as normal controls (age, 41-70 years; mean age, 55.42 ± 7.28 years). Peripheral blood samples (10 ml) from both patients with UCEC and healthy individuals

were collected, followed by centrifugation at $3,000 \times g$ for 10 min at 4°C within 4 h to obtain plasma supernatant. The collected plasma samples were further subjected to centrifugation at $16,000 \times g$ for 10 min at 4°C and subsequently stored at -80°C until further use. The present study adhered to the principles outlined in the Declaration of Helsinki, and ethical approval was obtained from Renmin Hospital of Wuhan University Ethics Committee (approval no. WDRY2023-K161). All participants signed a written informed consent form.

Cell culture. Procell Life Science & Technology, Ltd. provided two UCEC cell lines (HEC-1-A and Ishikawa). HEC-1-A and Ishikawa cells were grown in RPMI-1640 medium (Gibco; Thermo Fisher Scientific, Inc.) with 10% FBS (Gibco; Thermo Fisher Scientific, Inc.) and 1% penicillin/streptomycin (Invitrogen; Thermo Fisher Scientific, Inc.), with an environment with 5% CO_2 and a temperature of 37°C . Cells in the logarithmic growth phase were used for the subsequent experiments.

Cell transfection. miR-32-5p-inhibitor, miR-32-5p inhibitor-negative control (NC), overexpression (OE)-Forkhead Box N2 (FOXN2), OE-NC, miR-32-5p-mimic and miR-32-5p-mimic-NC were synthesized by Ribo Biotech, Ltd. The vector used for the overexpression transfections was pcDNATM 3.1⁽⁺⁾ (Invitrogen; Thermo Fisher Scientific, Inc.). Lipofectamine[®] 3000 (Invitrogen; Thermo Fisher Scientific, Inc.), HEC-1-A cells were transfected with miR-32-5p-inhibitor or miR-32-5p inhibitor-NC, while Ishikawa cells were transfected with miR-32-5p-mimic or miR-32-5p-mimic-NC. The concentration of nucleic acid used was 50 nM; the transfection process lasted for 48 h at 37°C , after which the cells were collected further functional experiments. The sequences of the miRNA mimic and inhibitors as well as those of the negative controls are listed in Table I.

Exosome isolation and characterization. Exosomes from UCEC plasma samples (UCEC-Exo) and normal controls (Normal-Exo) were isolated using an ExoQuickTM Exosome Precipitation Kit (System Biosciences, LLC) according to the manufacturer's instructions. Briefly, plasma samples ($500 \mu\text{l}$) were combined with exosome precipitation reagent ($100 \mu\text{l}$) and incubated at room temperature for 10 min. The mixture was then subjected to centrifugation at a speed of $10,000 \times g$ for a duration of 10 min at 4°C . The resulting pellet containing the exosomes was subsequently resuspended in PBS for subsequent analysis.

To isolate exosomes from the UCEC cell lines (HEC-1-A-Exo and Ishikawa-Exo), HEC-1-A or Ishikawa cells were cultured in RPMI-1640 medium supplemented with 10% FBS, at a temperature of 37°C at 5% CO_2 . Following a culture period of 72 h, the supernatant containing exosomes and cellular debris was separated using centrifugation ($10,000 \times g$ for 30 min at 4°C). Exosomes from the collected supernatant were extracted using the GMTM Exosome Isolation Reagent kit (Guangzhou Genesee Biotech. Co., Ltd.). The resulting mixture was incubated at a temperature of 4°C for 30 min before centrifugation at $2,000 \times g$ for 30 min. Finally, the isolated exosomes were PBS-resuspended for further analysis.

Table I. Sequences of the miRNA mimic and inhibitor.

Gene	Sequences (5'-3')
miR-32-5p-mimic	S: UAUUGCACAUUACUAAGUUGCA AS: CAACUUAGUAAUGUGCAAUAUU
miR-32-5p-mimic-NC	S: UUCUCCGAACGUGUCACGU AS: GUGACACGUUCGGAGAAUU
miR-32-5p-inhibitor	UGCAACUUAGUAAUGUGCAAUA
miR-32-5p-inhibitor-NC	ACGUGACACGUUCGGAGAA

miR, microRNA; NC, negative control; S, sense; AS, antisense.

Exosome structure was analyzed using transmission electron microscopy (TEM; Hitachi, Ltd.) as previously described (23). Nanoparticle tracking analysis (NTA) was conducted using the NanoSight NS300 (Malvern Panalytical, Ltd.) to analyze the size distribution of the isolated exosomes. Western blotting was utilized to identify the presence of exosomal indicators, including CD9, CD81, tumor susceptibility gene 101 (TSG101) and calnexin.

Co-culture system construction. The HEC-1-A donor cells (transfected with miR-32-5p-inhibitor-NC or miR-32-5p inhibitor) or Ishikawa donor cells (transfected with miR-32-5p-mimic-NC or miR-32-5p mimic) were seeded on a Transwell polyester permeable support. Simultaneously, the receptor HEC-1-A or Ishikawa cells (both untransfected) were cultured in the lower chamber of Transwell culture plate. After a 24 h incubation, the receptor cells were collected for subsequent experiments.

Quantitative reverse transcription-PCR (qRT-PCR). TRIzol (Invitrogen; Thermo Fisher Scientific, Inc.) was used for RNA isolation from UCEC cell lines according to the manufacturer's instructions. The Multi-type Sample DNA/RNA Extraction-Purification Kit (Sansure Biotech, Inc.) was used to isolate RNA from exosomes according to the manufacturer's instructions. The RNA concentration was measured using a Nanodrop spectrophotometer (Thermo Fisher Scientific, Inc.). The optical density 260/280 nm ratios of all RNA samples were ≥ 1.8 . cDNA was obtained using the ReverTra Ace qPCR RT Kit (Toyobo Co., Ltd.) according to the manufacturer's instructions and subject to PCR analysis using a SYBR High-Sensitivity qPCR Supermix Kit (Novoprotein Scientific, Inc.) with the Real-time PCR System (Applied Biosystems; Thermo Fisher Scientific, Inc.). The following thermocycling conditions were used for the PCR: Initial denaturation at 95°C for 10 min; 40 cycles of 95°C for 15 sec and 60°C for 30 sec. The $2^{-\Delta\Delta C_q}$ values (24) reflected the RNA expression levels using U6 (for miR-32-5p) (25,26) and GAPDH (for AKT, PI3K, Bcl-2 and FOXN2) as controls. qPCR primers used are shown in Table II.

Cell proliferation assays. The viability of UCEC cells was measured via CCK-8 assay. HEC-1-A or Ishikawa cells (3×10^3 cells/ml) were grown in 96-well plates for 0, 24, 48

and 72 h before adding the CCK-8 solution (15 μ l; Dojindo Laboratories, Inc.). Following a 2 h incubation, UCEC cell viability was calculated via microplate reader (Bio-Rad Laboratories, Inc.), with the absorbance at a wavelength of 450 nm.

Colony forming experiments were carried out to further estimate the proliferative capacities. HEC-1-A or Ishikawa cells (~1,000 cells) were seeded into each well of 6-well plates and cultured for 2 weeks. The culture medium was refreshed biweekly. Following that, the cells were rinsed with PBS, treated with 100 % methanol for fixation at 25°C for 10 min and subsequently dyed with 0.1% crystal violet (Sigma-Adrich; Merck KGaA) for a duration of 20 min at 25°C. Cells were then washed three times, and cell colonies were counted using a light microscope (Olympus Corporation).

The 5-ethynyl-2'-deoxyuridine (EdU) proliferation assay Kit (Abcam) was used according to the manufacturer's instructions. HEC-1-A or Ishikawa cells were initially incubated with 50 μ M EdU at 37°C for 2 h. Fixation was performed using 4% formaldehyde at 25°C for 15 min and permeabilized with 0.5% Triton X-100 at 25°C for 20 min. Following this, the cells were incubated with an Apollo reaction cocktail (1X; Abcam) at room temperature for ~30 min. To visualize DNA, cells were stained with DAPI at 25°C for 30 min. A fluorescence microscope (Carl Zeiss AG) was utilized to observe the EdU-positive cells.

Transwell migration assay. The upper chamber of the Transwell insert was pre-coated with 50 μ l of Matrigel at 37°C for 30 min, which had been diluted 5-fold in serum-free RPMI-1640. HEC-1-A or Ishikawa cells (5×10^4 cells) were suspended in a RPMI-1640 medium without serum and then placed into the upper chamber. Simultaneously, the lower chamber was supplemented with RPMI-1640 medium containing 10% FBS. Following overnight incubation at 37°C, the cells in the lower chamber were treated with 0.1% crystal violet at 37°C for 15 min. Images of the stained cells were captured using a light microscope (magnification, x400).

Flow cytometry analysis. The apoptotic UCEC cells were assessed by utilizing the Annexin V-FITC apoptosis detection kit (Thermo Fisher Scientific, Inc.) following the guidelines provided by the manufacturer. The HEC-1-A or Ishikawa cells (2×10^5) were suspended in 500 μ l of binding buffer and then treated with Annexin V-EGFP and PI (5 μ l each) at a

Table II. PCR primer list.

Gene	Sequences (5'-3')	Accession no.
miR-32-5p	F: ACACTCCAGCTGGGTATTGCACATTACTAA R: TGGTGTCTGGAGTCG	NC_000009.12
miR-32-5p stem-loop primer ^a	CTCAACTGGTGTCTGGAGTCGGCAATTCAGTTGAGTGCAACTT	
U6	F: CTCGCTTCGGCAGCACACA R: AACGCTTCACGAATTGTGCGT	NC_000015.10
AKT	F: AGAAGCAGGAGGAGGAGGAG R: TCTCCTTCACCAGGATCACC	NM_005163.2
PI3K	F: CCACGACCATCATCAGGTGAA R: CCTCACGGAGGCATTCTAAAGT	NM_006218.4
Bcl-2	F: GAGGATTGTGGCCTTCTTTG R: ACAGTTCCACAAAGGCATCC	NM_000633.3
FOXN2	F: CCAGGTCTAGCGTGTCTTCC R: AGCCACTGTCTCCAAGAGGA	NM_001375442.1
GAPDH	F: ACAACTTTGGTATCGTGGAAGG R: GCCATCACGCCACAGTTTC	NM_002046.7

^aUsed for reverse transcription. F, forward; R, reverse; miR, microRNA; FOXN2, Forkhead Box N2.

temperature of 4°C for a duration of 15 min in the absence of light. Thereafter, the apoptosis of the cells was evaluated using a FACScan flow cytometer (Becton, Dickinson and Company) and analyzed using the BD CellQuest software (version 3.3; Becton, Dickinson and Company).

Target prediction. The mRNA targets of miR-32-5p were predicted using the StarBase software (version 2.0; <https://starbase.sysu.edu.cn/>), and 2,143 targets were predicted. FOXN2 was selected for the subsequent experiments due to its key role in endometrial cancer (27) and unknown regulatory relationship with miR-32-5p.

Dual luciferase reporter (DLR) assay. The 3'-untranslated region (UTR) of FOXN2 containing the putative binding sites of miR-32-5p was cloned into the luciferase reporter plasmid pGL3 vector (Promega Corporation) to construct the FOXN2 wild-type (WT)/mutant type (MUT). Ishikawa cells (5×10^3) were seeded onto a 24-well plate and co-transfected with one of the aforementioned plasmids (80 ng), along with either miR-32-5p mimic or mimic-NC (10 nM), using Lipofectamine[®] 3000 (Invitrogen; Thermo Fisher Scientific, Inc.). After 48 h at 37°C, the relative luciferase activity was determined using a Dual-Luciferase Reporter Assay System Kit (Promega Corporation). The activity of firefly luciferase was normalized to that of *Renilla* luciferase.

Western blotting. RIPA lysis buffer (Beyotime Institute of Biotechnology) containing protease inhibitors was utilized for protein extraction from cells, and protein concentrations were determined using the BCA Protein Assay Kit (Beyotime Institute of Biotechnology). In each lane, ~30 µg of proteins was separated using 10% SDS-PAGE and transferred onto a PVDF membrane. Blocking of the membrane was carried

out at room temperature using 5% bovine serum albumin (Beyotime Institute of Biotechnology) for 2 h at 25°C. Afterward, the membrane was placed in a 4°C environment and incubated overnight with primary antibodies against AKT (1:1,500; cat. no. #9272; Cell Signaling Technology), p-AKT (1:1,500; cat. no. #4060; Cell Signaling Technology), PI3K (1:1,500; cat. no. #4249; Cell Signaling Technology), Bcl-2 (1:1,500; cat. no. #3498; Cell Signaling Technology), FOXN2 (1:1,500; cat. no. ab236385; Abcam), GAPDH (1:1,500; cat. no. #2118; Cell Signaling Technology), Calnexin (1:1,500; cat. no. #2679; Cell Signaling Technology), CD9 (1:1,500; cat. no. #13174; Cell Signaling Technology), CD81 (1:1,500; cat. no. ab79559; Abcam) and TSG101 (1:1,500; cat. no. ab125011; Abcam). Subsequently, the membranes were washed three times using tris-buffered saline with 0.05% Tween 20. Then, the HRP-conjugated secondary antibody (1:3,000; cat. no. #7074; Cell Signaling Technology) was added at room temperature for 1 h. The reference gene used was GAPDH. The immunoreactive protein bands were observed using an ECL Basic Kit (ABclonal Biotech Co., Ltd.) using a Gel-Pro analyzer (version 4.0; Media Cybernetics, Inc.).

Statistical analysis. Data analysis was conducted utilizing SPSS software (version 20.0; IBM Corp.). The findings were presented as the mean value ± standard deviation. Student's t-test (unpaired) or one-way ANOVA with Tukey's post hoc test was used for comparisons. Multivariate Cox regression analysis was performed on DE-miRNAs utilizing the Survival package in R (Posit Software, PBC). The median was selected as the cut-off value, and Kaplan-Meier survival curves were generated using the Survminer package (version 0.5.0; DataNovia) and analyzed using log-rank test. P<0.05 was considered to indicate a statistically significant difference.

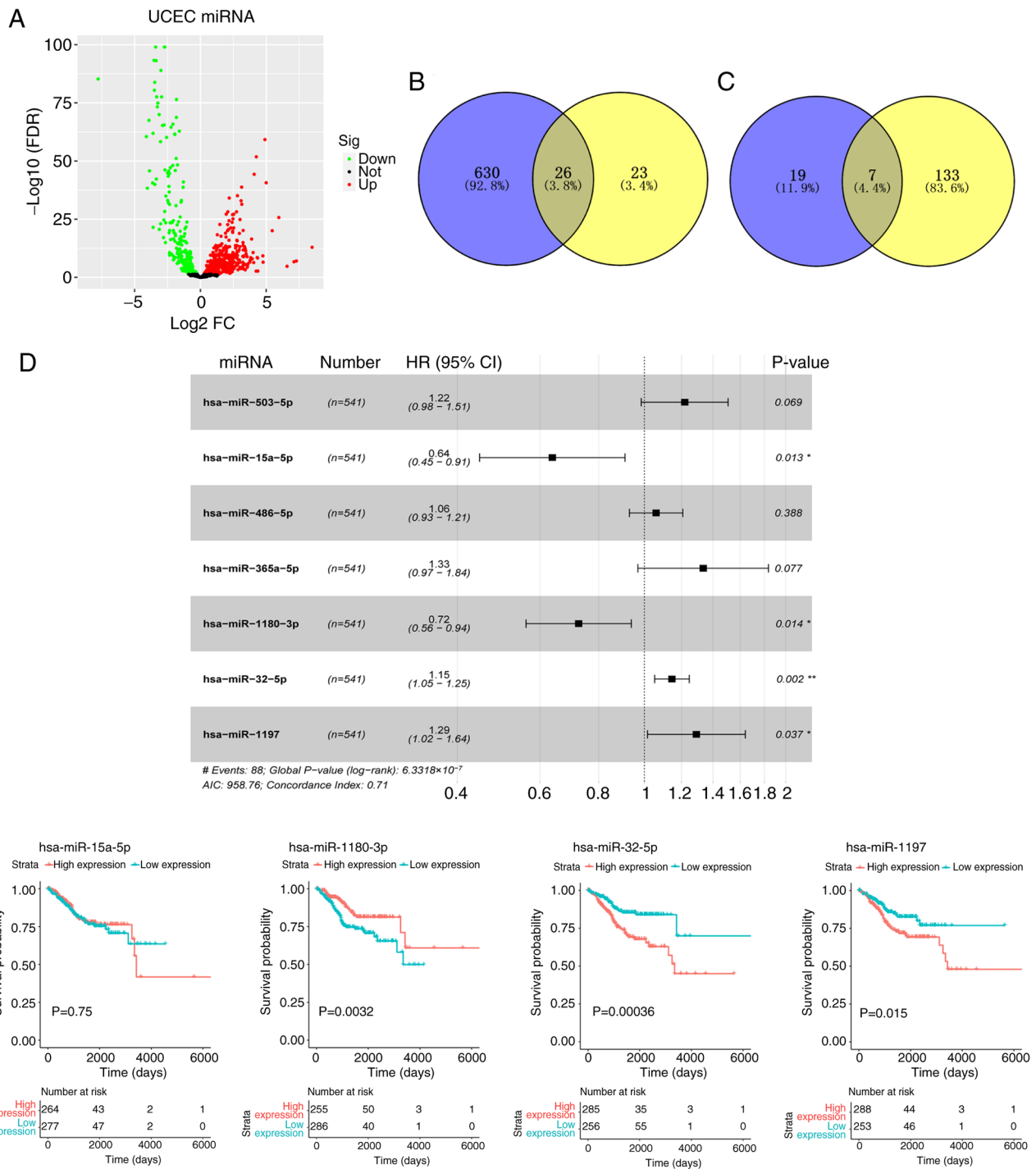


Figure 1. miRNA screening. (A) The volcano plot of DE-miRNAs (n=656) comparing normal and UCEC samples from TCGA database. Green represents 402 miRNAs that were differentially upregulated in UCEC samples; red represents 254 miRNAs that were differentially downregulated. (B) The intersection of the 656 DE-miRNAs with the 49 DE-miRNAs analyzed by Zhou *et al* (21), 26 DE-miRNAs were identified. (C) From the univariate Cox risk regression analysis, 140 miRNAs were screened as prognostic miRNAs in patients with UCEC. The selected 140 miRNAs were intersected with 26 DE-miRNAs, from which 7 DE-miRNAs were obtained. (D) Multivariate Cox regression analysis was used to determine the independent prognostic factors of UCEC. (E) Survival probability analysis for miR-15a-5p, miR-1180-3p, miR-32-5p and miR-1197. DE, differentially expressed; UCEC, uterine corpus endometrial carcinoma; miRNA, microRNA. AIC, Akaike Information Criterion.

Results

miRNA screening. The present study screened miRNA expression data from patients with UCEC of TCGA database and DE-miRNA data from Zhou *et al* (21). Compared with that in normal samples, there were 656 miRNAs differentially expressed in UCEC tissues from TCGA database (Fig. 1A).

Among them, 402 miRNAs were differentially upregulated, while 254 miRNAs were differentially downregulated in UCEC. The heatmap of top 50 DE-miRNAs is shown in Fig. S1. Through intersecting these 656 DE-miRNAs with DE-miRNA data (comprising 49 DE-miRNAs) from Zhou *et al* (21), a total of 26 DE-miRNAs were obtained (Fig. 1B). Univariate Cox risk regression analysis (P<0.05) was conducted on the TCGA

data, and 140 miRNAs were identified as potential prognostic miRNAs in patients with UCEC. These 140 miRNAs were then intersected with 26 DE-miRNAs from the aforementioned analysis, from which 7 overlapping DE-miRNAs were identified (Fig. 1C). Multivariate Cox regression analysis was used to demonstrate that miR-15a-5p ($P=0.013$), miR-1180-3p ($P=0.014$), miR-32-5p ($P=0.002$) and miR-1197 ($P=0.037$) were independent prognostic factors of UCEC (Fig. 1D). Survival probability analysis was conducted to investigate the effects of the expression of these four miRNAs on survival outcomes, from which miR-32-5p demonstrated the most significant effects on survival probability and was therefore selected for further investigation ($P=0.00036$; Fig. 1E).

miR-32-5p is overexpressed in UCEC-Exo. To confirm the successful isolation of exosomes from plasma samples from patients with UCEC and healthy controls, TEM and NTA were employed to characterize the isolated exosomes. The isolated vesicles exhibited a double-layered membrane structure and a size distribution of ~100 nm in diameter, which were in accordance with the expected characteristics of exosomes (Fig. 2A and B) (28). Western blotting demonstrated that the vesicles expressed the exosome-positive markers CD9, CD81 and TSG101, while the exosome-negative marker, Calnexin, was absent in the isolated vesicles (Fig. 2C), which demonstrated successful isolation of exosomes. The expression of miR-32-5p in normal-Exo and UCEC-Exo was then determined; miR-32-5p expression was upregulated in UCEC-Exo compared with that of normal-Exo ($P<0.05$; Fig. 2D).

Expression of miR-32-5p in exosomes isolated from UCEC cell lines. Subsequently, exosomes were isolated from two UCEC cell lines (HEC-1-A and Ishikawa). The characteristics of vesicles from UCEC cell lines were similar to exosomes isolated from plasma samples (Fig. 3A and B). Western blotting demonstrated presence of exosome-positive markers CD9, CD81 and TSG101 in the exosomes-enriched fractions, and absence of Calnexin (Fig. 3C). Additionally, compared with that of HEC-1-A-Exo, miR-32-5p expression was downregulated in Ishikawa-Exo ($P<0.001$; Fig. 3D).

miR-32-5p affects the proliferative capacities, migratory abilities and apoptotic rate of UCEC cells. miR-32-5p expression levels were significantly reduced in Ishikawa cells compared with that of HEC-1-A cells ($P<0.001$; Fig. 4A). As miR-32-5p demonstrated high expression levels in HEC-1-A cells, they were selected for transfection with the miR-32-5p inhibitor to achieve interference in miR-32-5p expression, whereas the Ishikawa cells were chosen for transfection with the miR-32-5p mimic to achieve overexpression, due to the low expression levels of miR-32-5p in Ishikawa cells. qRT-PCR results that miR-32-5p expression in HEC-1-A cells was significantly decreased following transfection with the miR-32-5p inhibitor ($P<0.001$), while miR-32-5p was overexpressed in Ishikawa cells upon transfection with the miR-32-5p mimic (Fig. 4B; $P<0.001$). miR-32-5p inhibition significantly suppressed the viability of HEC-1-A cells, as evidenced by a CCK-8 assay (Fig. 4C; $P<0.001$). Conversely, overexpression of miR-32-5p increased the cell viability of Ishikawa cells

(Fig. 4C; $P<0.001$). Colony formation and EdU proliferation assays further confirmed the impacts of miR-32-5p expression status on cell proliferation. Transfection with miR-32-5p inhibitor led to a significant decrease in colony formation efficiency and the percentages of EdU-positive cells in HEC-1-A cells (Fig. 4D and E; $P<0.05$), while transfection with miR-32-5p mimic significantly increased colony formation efficiency and EdU-positive cell percentages in Ishikawa cells ($P<0.01$). The migratory abilities of UCEC cell were assessed using a Transwell assay, demonstrating that down-regulation of miR-32-5p significantly suppressed HEC-1-A cell migration (Fig. 4F; $P<0.01$), whereas miR-32-5p overexpression significantly increased the migratory capacities of Ishikawa cells ($P<0.01$). Furthermore, flow cytometry analysis demonstrated increased apoptosis in HEC-1-A cells upon treatment with miR-32-5p inhibitor (Fig. 4G; $P<0.001$), while Ishikawa cells exhibited a significantly reduced apoptotic rate following treatment with miR-32-5p mimic ($P<0.001$).

miR-32-5p negatively regulates FOXN2 and activates PI3K/AKT/Bcl-2 pathway. The Starbase software predicted a potential binding site between miR-32-5p and FOXN2 (Fig. 5A). The DLR assay was conducted in Ishikawa cells, which demonstrated a significant decrease in relative luciferase activity in the FOXN2-WT + miR-32-5p mimic group when compared with that of the FOXN2-WT + mimic-NC group (Fig. 5B; $P<0.001$), while no statistical changes were observed between the FOXN2-MUT + miR-32-5p mimic and FOXN2-MUT + mimic-NC groups. These findings suggested that FOXN2 was a direct target of miR-32-5p. The PI3K/AKT pathway is a well-established mechanism implicated in the promotion of cancer development (29,30), including in UCEC (31), but whether it is regulated by miR-32-5p in UCEC remains unknown. Therefore, we further explored the effects of miR-32-5p on PI3K/AKT pathway in UCEC cells. Inhibition of miR-32-5p resulted in a significant inhibition of AKT and PI3K mRNA expression (Fig. 5C; $P<0.001$). Additionally, significantly decreased Bcl-2 mRNA expression levels ($P<0.05$) and increased FOXN2 mRNA expression levels ($P<0.01$) were observed upon miR-32-5p inhibition. The opposite effects were observed in the results of mRNA expression of AKT, PI3K, Bcl-2 and FOXN2 in Ishikawa cells following transfection of miR-32-5p mimic (Fig. 5D; $P<0.05$). Western blotting was used to assess protein levels in HEC-1-A and Ishikawa cells. The expression levels of AKT protein were unaltered by both miR-32-5p overexpression and inhibition (Fig. 5E and F). When transfected with miR-32-5p inhibitor in HEC-1-A cells, the protein expression levels of p-AKT, PI3K and Bcl-2 were significantly decreased ($P<0.05$), but FOXN2 protein expression levels were increased ($P<0.001$). The ratio of p-AKT/AKT was significantly decreased in HEC-1-A cells transfected with miR-32-5p-inhibitor ($P<0.001$). However, overexpression with miR-32-5p mimic showed the opposite effects ($P<0.05$). These findings suggested that miR-32-5p negatively regulated FOXN2 and activated PI3K/AKT/Bcl-2 pathway. Rescue experiments were performed in Ishikawa cells to further verify the effects of miR-32-5p-mediated FOXN2 on PI3K/AKT/Bcl-2 pathway. mRNA expression of

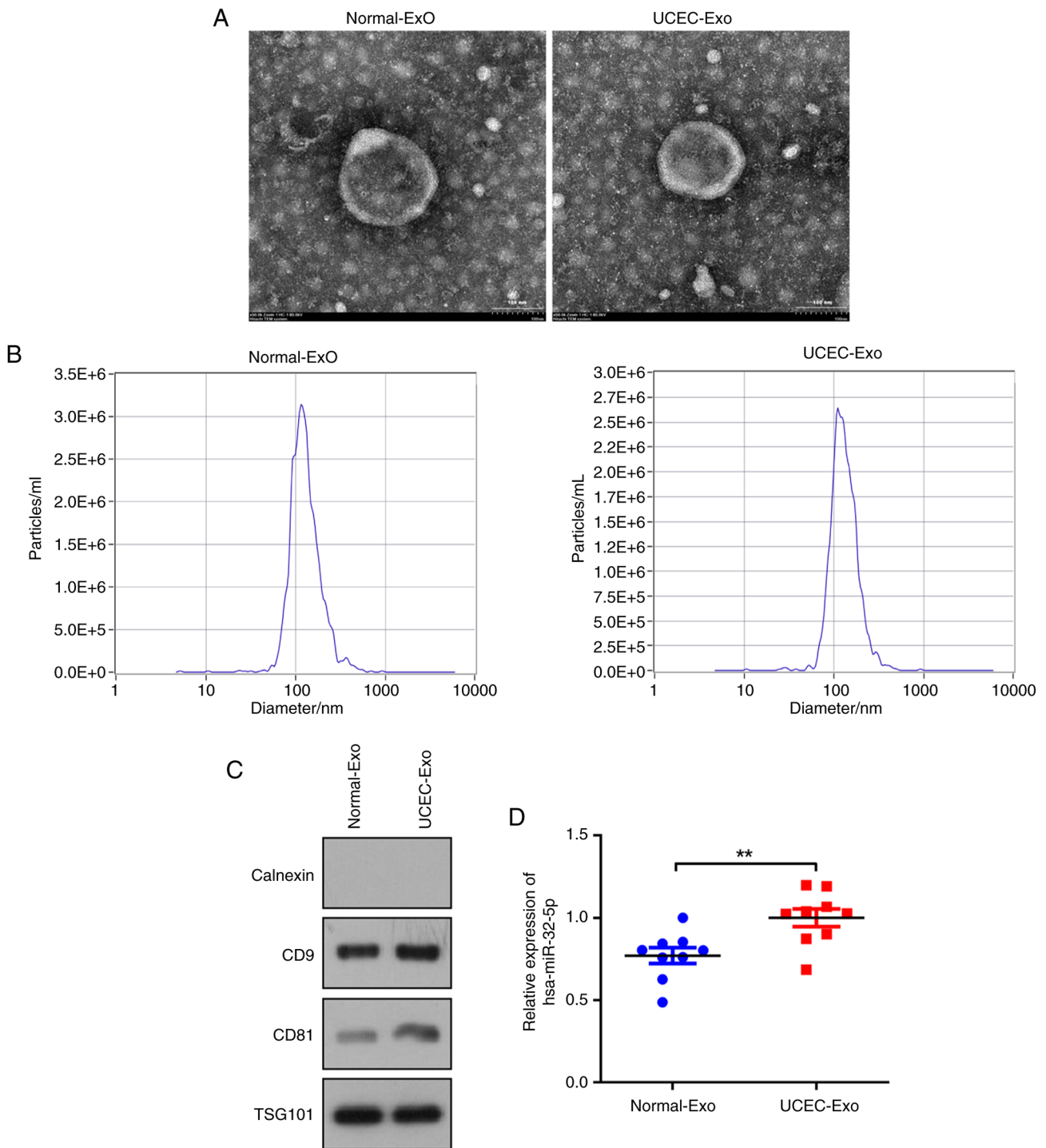


Figure 2. miR-32-5p is overexpressed in UCEC-Exo. (A) The morphology of plasma exosomes was visualized using transmission electron microscopy. Scale bar, 100 μ m. (B) The size distribution and concentration of plasma exosomes were assessed by nanoparticle tracking analysis. The X-axis represents the diameter (nm) of exosomes, while the Y-axis represents the concentration of exosomes. (C) The protein levels of exosome-positive markers (CD9, CD81 and TSG101) and exosome-negative marker (Calnexin) in plasma exosomes were determined using western blotting. (D) The expression of miR-32-5p in normal-Exo and UCEC-Exo was assessed using quantitative reverse transcription-PCR. **P<0.01 vs. normal-Exo. UCEC, uterine corpus endometrial carcinoma; miRNA, microRNA; Exo, exosome; TSG101, tumor susceptibility gene 101.

FOXN2 was significantly increased followed transfection of OE-FOXN2 (Fig. 6A; P<0.0001), which demonstrated the successful transfection. Overexpression of FOXN2 significantly reversed the effects of miR-32-5p-mimic transfection that promoted the activation of PI3K/AKT/Bcl-2 pathway (Fig. 6B and C; P<0.05), and the inhibitory effect on FOXN2 expression levels (Fig. 6B and C; P<0.001).

Exo-miR-32-5p regulates the proliferation, migration and apoptosis of UCEC cells through regulating FOXN2 expression and PI3K/AKT/Bcl-2 pathway. The impacts of Exo-miR-32-5p on the proliferation, migration and apoptosis of UCEC cells were examined utilizing a co-culture model. Firstly, Exo-miR-32-5p expression in HEC-1-A cells transfected with miR-32-5p-inhibitor or in Ishikawa cells

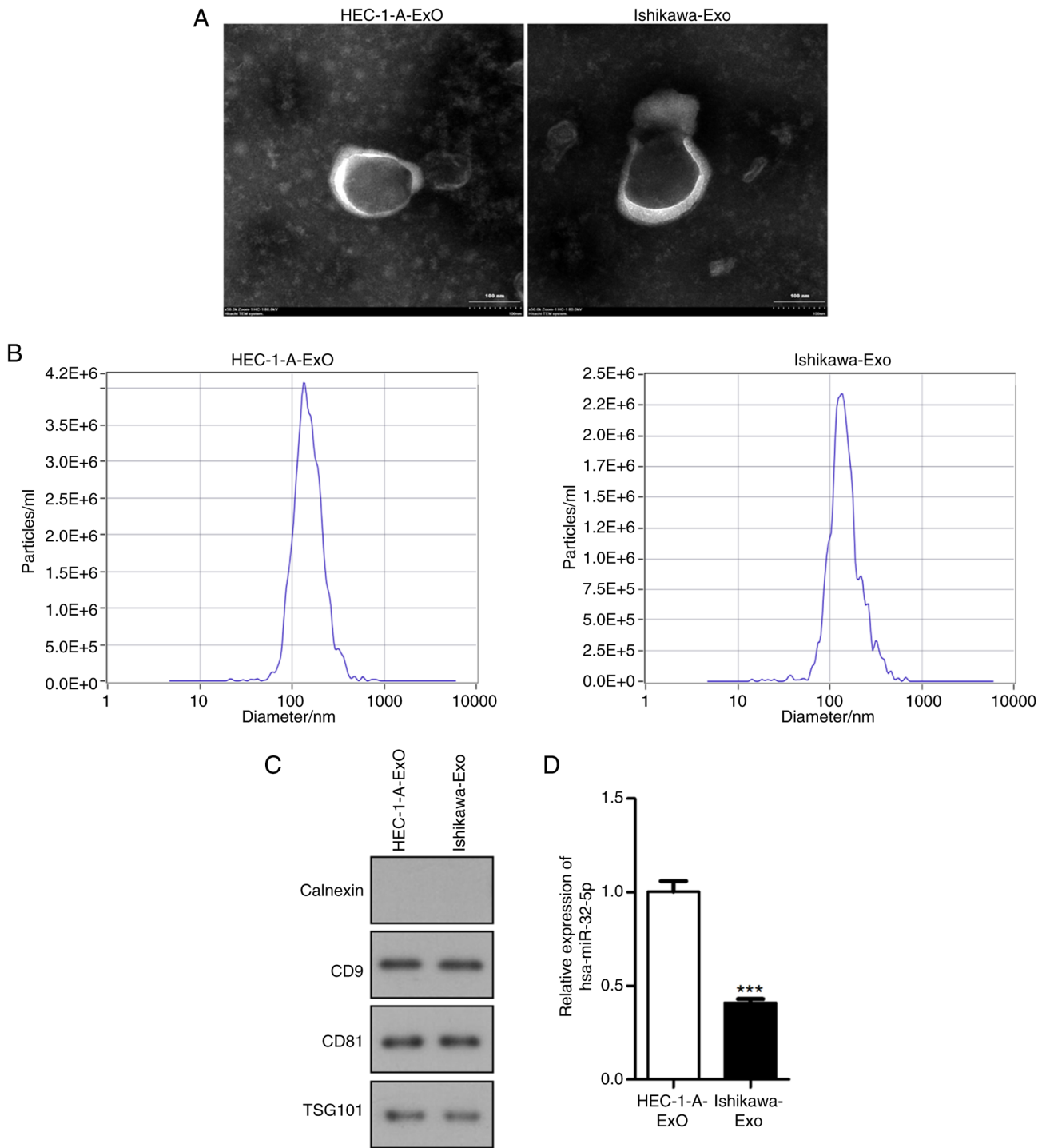


Figure 3. Expression of miR-32-5p in exosomes isolated from UCEC cell lines. (A) The morphology of UCEC cell line-derived exosomes was visualized using transmission electron microscopy. Scale bar, 100 μ m. (B) The size distribution and concentration of UCEC cell line-derived exosomes were assessed by nanoparticle tracking analysis. The X-axis represents the diameter (nm) of exosomes, while Y-axis represents the concentration of exosomes. (C) The protein levels of exosome-positive markers (CD9, CD81 and TSG101) and exosome-negative marker (Calnexin) in UCEC cell line-derived exosomes were determined using western blotting. (D) The expression of miR-32-5p in HEC-1-A-Exo and Ishikawa-Exo was detected using quantitative reverse transcription-PCR. *** $P < 0.001$ vs. HEC-1-A-Exo. UCEC, uterine corpus endometrial carcinoma; miRNA, microRNA; Exo, exosome; TSG101, tumor susceptibility gene 101.

transfected with miR-32-5p-mimic was determined using qRT-PCR. miR-32-5p expression was significantly down-regulated in Exo-miR-32-5p-inhibitor group when compared with the Exo-miR-32-5p-inhibitor-NC group (Fig. 7A; $P < 0.001$), while miR-32-5p expression levels were significantly increased in the Exo-miR-32-5p-mimic group when compared with the Exo-miR-32-5p-mimic-NC group (Fig. 7A;

$P < 0.001$). Compared with the Exo-miR-32-5p-inhibitor-NC group, the proliferation and migration of HEC-1-A cells were significantly decreased in the Exo-miR-32-5p-inhibitor group (Fig. 7B-E; $P < 0.01$), while the rate of apoptosis was increased (Fig. 7F; $P < 0.001$). Conversely, compared with the Exo-miR-32-5p-mimic-NC group, a significant increase of proliferative and migratory capacities (Fig. 7B-E; $P < 0.01$) and

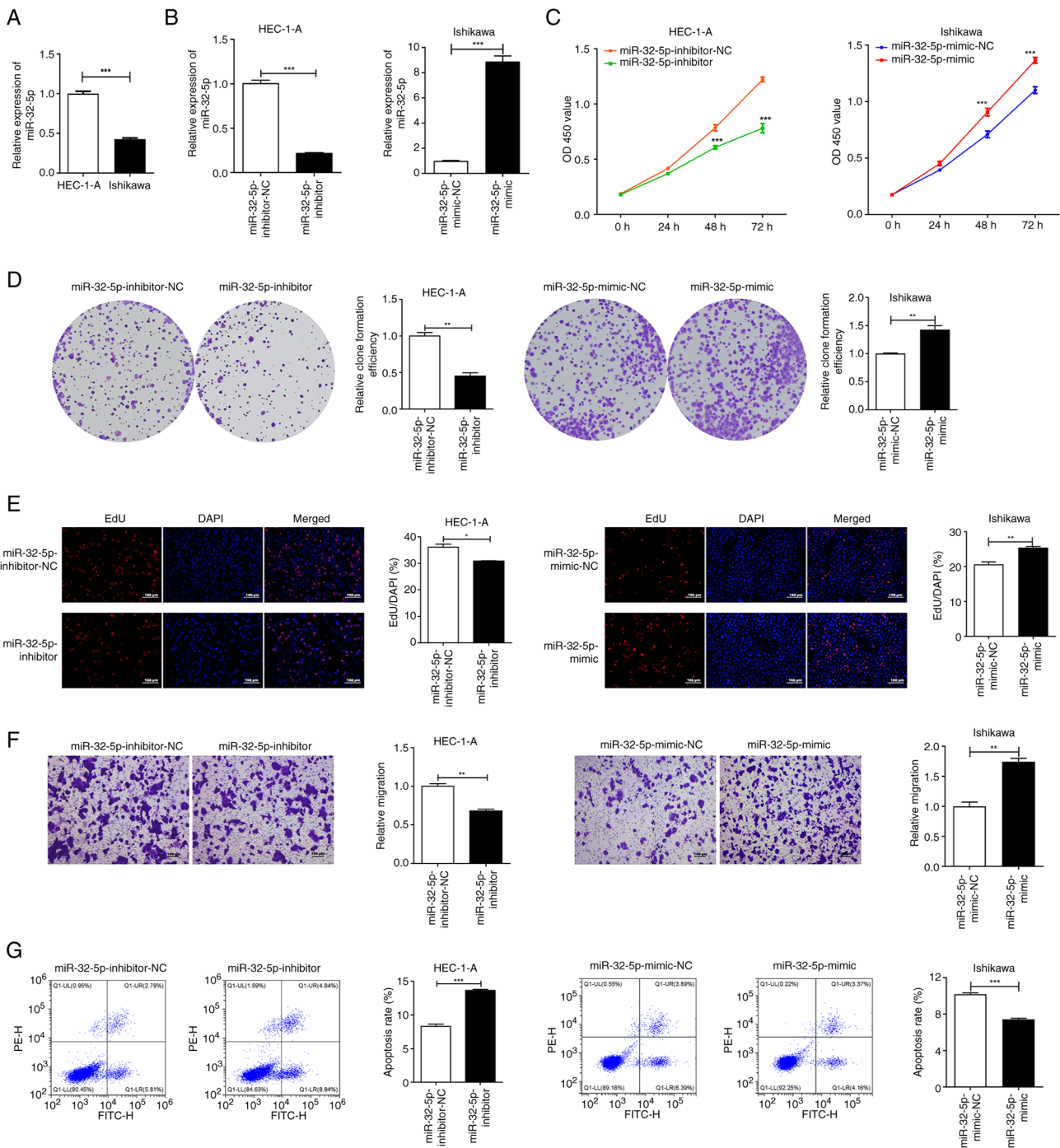


Figure 4. Effects of miR-32-5p on the proliferative capacities, migratory abilities and apoptotic rate of UCEC cells. (A) The expression of miR-32-5p in HEC-1-A and Ishikawa cells were then determined using quantitative reverse transcription-PCR. ***P<0.001 vs. HEC-1-A cells. (B) The expression of miR-32-5p in HEC-1-A cells after transfection of miR-32-5p inhibitor or in Ishikawa cells after transfection of miR-32-5p mimic. (C) The viability of UCEC cell lines were measured using the CCK-8 assay. (D) Relative colony formation efficiency of UCEC cell lines was evaluated using the colony formation assay. (E) EdU-positive cells were measured through EdU proliferation assay. (Scale bar, 100 μ m). (F) The migratory potential of UCEC cell lines were determined via Transwell migration assay. (Scale bar, 100 μ m). (G) Flow cytometry was used to detect apoptosis. *P<0.05, **P<0.01, ***P<0.001 vs. miR-32-5p inhibitor-NC or miR-32-5p mimic-NC. UCEC, uterine corpus endometrial carcinoma; miRNA, microRNA; NC, negative control; EdU, 5-ethynyl-2'-deoxyuridine.

significant decrease of the apoptosis rate in Ishikawa cells of the Exo-miR-32-5p-mimic group was demonstrated (Fig. 7F; P<0.001). Additionally, FOXN2 levels were increased, Bcl-2 levels were decreased and the PI3K/AKT pathway was inactivated in HEC-1-A cells (Fig. 7G and H; P<0.01), while these effects were all reversed in Ishikawa cells (Fig. 7G and H; P<0.01).

Discussion

UCEC is a highly prevalent malignant tumor affecting the female reproductive system, particularly within obstetrics and gynecological tumors in Western countries (32). The incidence of UCEC has been progressively increasing in China, posing a significant threat to women's health (33). Diagnosis of UCEC

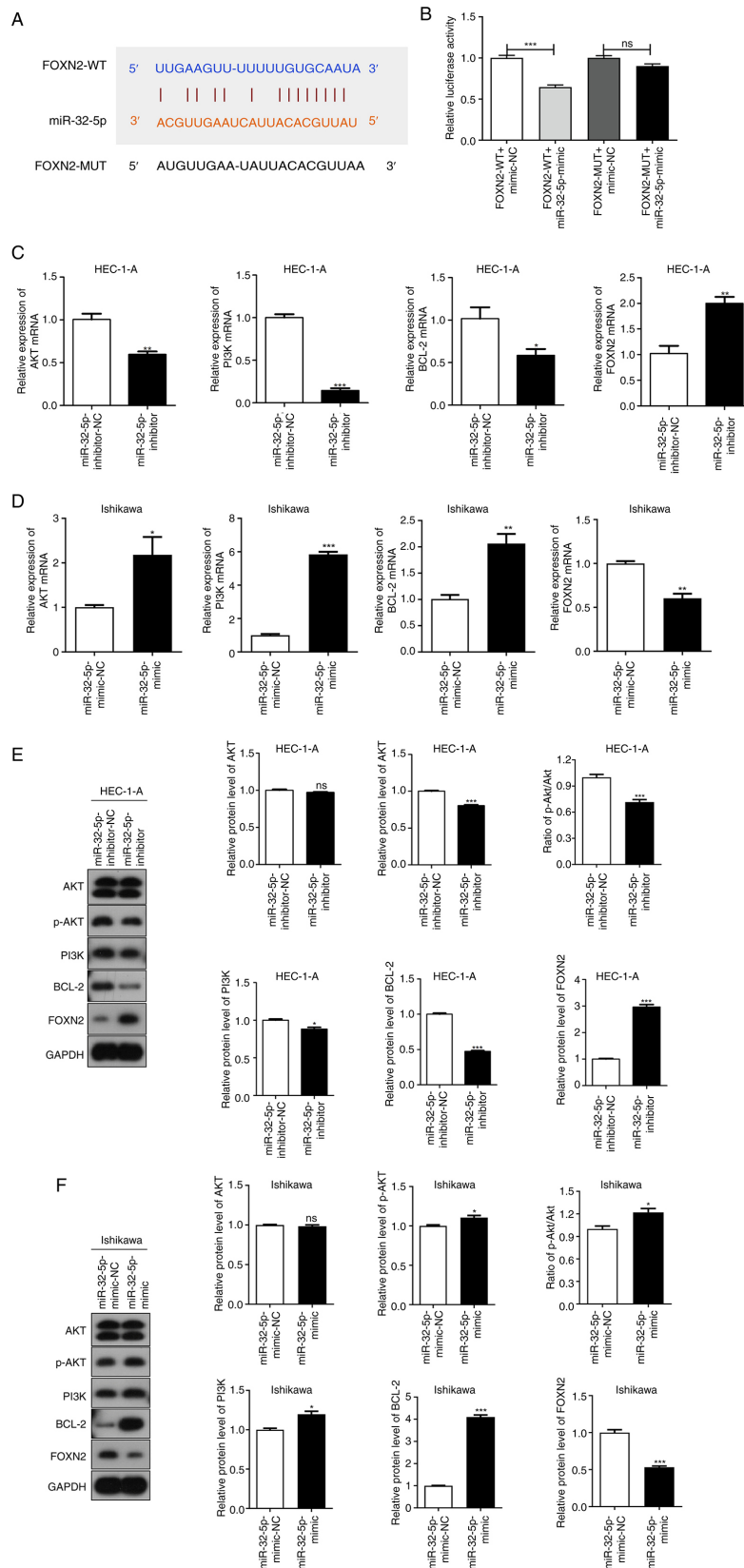


Figure 5. miR-32-5p negatively regulates FOXN2 and activates PI3K/AKT pathway. (A) The Starbase software shows the potential binding site for miR-32-5p and FOXN2. (B) A dual luciferase reporter assay was conducted to assess the relationship between miR-32-5p and FOXN2. *** $P < 0.001$ vs. FOXN2-WT + mimic-NC. (C) The mRNA expression of AKT, PI3K, Bcl-2 and FOXN2 in HEC-1-A cells transfected with miR-32-5p inhibitor or inhibitor-NC was detected using qRT-PCR. * $P < 0.05$, ** $P < 0.01$, *** $P < 0.001$ vs. miR-32-5p inhibitor-NC. (D) The mRNA expression of AKT, PI3K, Bcl-2 and FOXN2 in Ishikawa cells transfected with miR-32-5p mimic or mimic-NC was detected by qRT-PCR. * $P < 0.05$, ** $P < 0.01$ and *** $P < 0.001$ vs. miR-32-5p mimic-NC. (E) The protein levels of AKT, PI3K, p-AKT, Bcl-2, FOXN2 and the ratio of p-AKT/AKT in HEC-1-A cells transfected with miR-32-5p inhibitor or inhibitor-NC were measured using western blotting. * $P < 0.05$ and *** $P < 0.001$ vs. miR-32-5p inhibitor-NC. (F) The protein levels of AKT, PI3K, p-AKT, Bcl-2, FOXN2 and the ratio of p-AKT/AKT in Ishikawa cells transfected with miR-32-5p mimic or mimic-NC were measured using western blotting. * $P < 0.05$ and *** $P < 0.001$ vs. miR-32-5p inhibitor-NC. UCEC, uterine corpus endometrial carcinoma; miRNA, microRNA; NC, negative control; NS, not significant; WT, wild-type; MUT, mutant; qRT-PCR, quantitative reverse transcription-PCR; p-, phosphorylated; FOXN2, Forkhead Box N2.

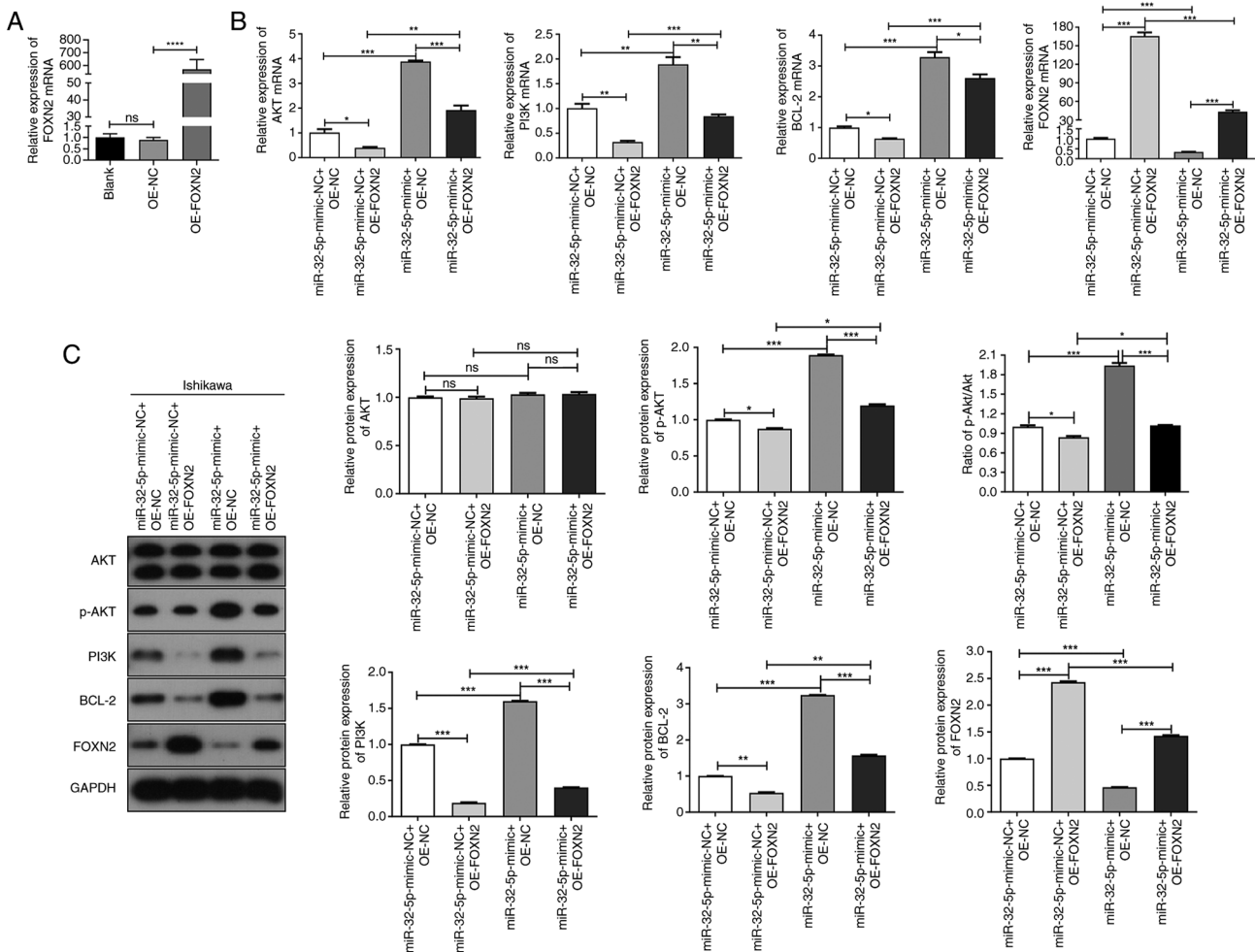


Figure 6. Effects of miR-32-5p-mediated FOXN2 on PI3K/AKT/Bcl-2 pathway. (A) Following transfection of OE-FOXN2/OE-NC in Ishikawa cells, the mRNA expression of FOXN2 was determined via qRT-PCR. Following transfection of miR-32-5p-mimic or OE-FOXN2 in Ishikawa cells, (B) the mRNA expression and (C) protein levels of FOXN2/PI3K/AKT/Bcl-2 and the ratio of p-AKT/AKT were determined through qRT-PCR and western blotting, respectively. *P<0.05, **P<0.01, ***P<0.001, ****P<0.0001. UCEC, uterine corpus endometrial carcinoma; miRNA, microRNA; NC, negative control; NS, not significant; WT, wild-type; MUT, mutant; qRT-PCR, quantitative reverse transcription-PCR; p-, phosphorylated; FOXN2, Forkhead Box N2; OE, overexpression.

typically relies on clinical symptoms, medical history and pathological findings. Patients are required to undergo uterine apexesis for pathology examination in order to accurately diagnose UCEC, as there is a lack of effective biomarkers (34). Exosomal miRNAs have gained significant attention in the field of precision medicine due to their non-invasive nature, accessibility and stability (35).

Previous research has demonstrated that exosomal miRNAs hold potential as effective biomarkers for cancer screening, diagnosis and monitoring purposes (36,37). In the present study, among the four candidate miRNAs, miR-32-5p was identified as the most significantly associated with the survival probability (P=0.00036) of patients with UCEC. Meanwhile, the role and mechanism of exosomal miR-32-5p in UCEC progression *in vitro* have been preliminarily elucidated, indicating that exosomal-miR-32-5p can regulate the proliferation, migration and apoptosis of UCEC cells through FOXN2/PI3K/AKT pathway.

miRNAs, a subclass of non-coding RNAs ranging from 19 to 25 nucleotides in length, serve key roles in extensive modulation by specifically targeting the 3'-UTRs of mRNAs (38). miR-32-5p, belonging to miR-32 family, is located on

chromosome 9 (39). Numerous studies have provided evidence for the functional significance of miR-32-5p in various cancer types, highlighting its capacity to modulate tumor development, growth patterns, metastatic potential and invasive characteristics. For example, overexpression of the long non-coding RNA GAS5 suppressed the proliferative and metastatic capacities of pancreatic cancer cells, while upregulation of miR-32-5p reversed this inhibitory effect (17). Notably high expression levels of miR-32-5p were observed in colorectal cancer tissues and strongly correlated with poor prognosis; however, miR-32-5p downregulation markedly impeded the metastasis of colorectal cancer cells (18). Additionally, upregulation of miR-32-5p expression has also been documented in gynecological malignancies such as ovarian cancer, and its overexpression significantly accelerated cancer cell growth and metastasis (19). In the present study, a significant increase level of miR-32-5p was identified in UCEC tissues in contrast to that of normal tissues, implying that miR-32-5p may be an onco-miRNA affecting the development of UCEC. miR-32-5p expression was then inhibited or overexpressed to further explore the dysregulation of miR-32-5p on the malignant behaviors of UCEC cells. High levels of miR-32-5p

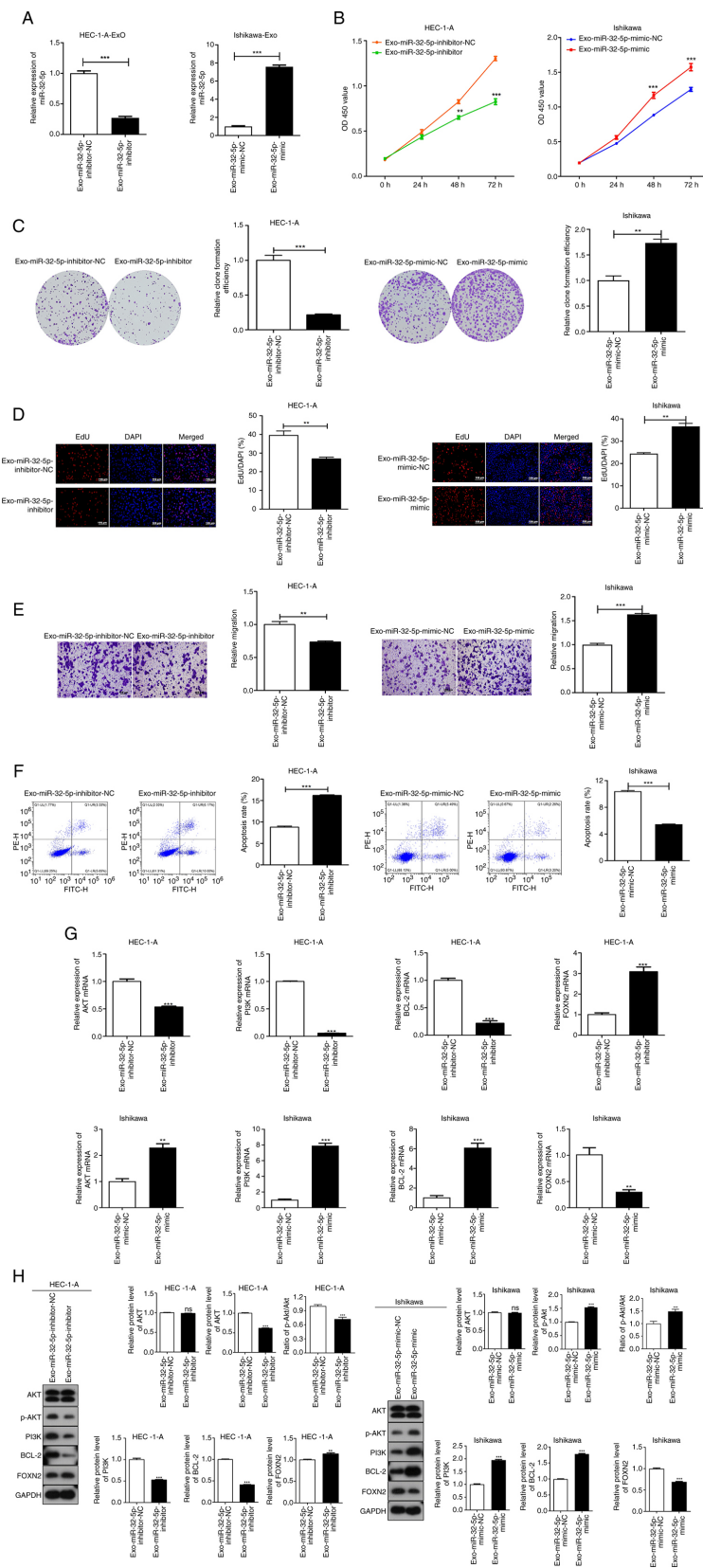


Figure 7. Exo-miR-32-5p regulates the proliferation, migration and apoptosis of UCEC cells through regulating FOXN2 expression and PI3K/AKT/Bcl-2 pathway. The impact of Exo-miR-32-5p on the proliferation, migration and apoptosis of UCEC cells were examined utilizing a co-culture model. (A) Exo-miR-32-5p expression in HEC-1-A cells transfected with miR-32-5p-inhibitor or in Ishikawa cells transfected with miR-32-5p-mimic was determined through qRT-PCR. (B) The viability of UCEC cell lines were measured using the CCK-8 assay. (C) Relative colony formation efficiency of UCEC cell lines was evaluated using the colony formation assay. (D) EdU-positive cells were measured through EdU proliferation assay. (Scale bar, 100 μ m). (E) The migratory potential of UCEC cell lines were determined via the Transwell migration assay. (F) Flow cytometry was used to detect apoptosis. (Scale bar, 100 μ m). (G) The migratory potential of UCEC cell lines were determined via the Transwell migration assay. (F) Flow cytometry was used to detect apoptosis. (G) The mRNA expression of AKT, PI3K, Bcl-2 and FOXN2 was detected by qRT-PCR. (H) The protein levels of AKT, PI3K, p-AKT, Bcl-2, FOXN2 and the ratio of p-AKT/AKT were measured by western blotting. ** $P < 0.01$, *** $P < 0.001$ vs. Exo-miR-32-5p inhibitor-NC or Exo-miR-32-5p mimic-NC. UCEC, uterine corpus endometrial carcinoma; miRNA, microRNA; NC, negative control; NS, not significant; WT, wild-type; MUT, mutant; qRT-PCR, quantitative reverse transcription-PCR; p-, phosphorylated; FOXN2, Forkhead Box N2; EdU, 5-ethynyl-2'-deoxyuridine.

expression were found to significantly increase the proliferative and migratory capacities, while concurrently suppressing the UCEC apoptosis rate. Meanwhile, inhibition of miR-32-5p yielded the opposite results. These findings further substantiate the present hypothesis that miR-32-5p can induce the progression of UCEC by enhancing cancer cell proliferation and migration, while inhibiting apoptosis.

Additionally, miR-32-5p has been reported to target the downstream mRNAs, exerting regulation effects in various human solid tumors, such as miR-32-5p-SIK1 in ovarian cancer (19), miR-32-5p-HOXB8 in cervical cancer (40) and miR-32-5p-TOB1 in breast cancer (41). Considering the regulatory function of miR-32-5p in UCEC cells, the existence of potential downstream genes modulated by miR-32-5p during UCEC progression could be considered. In the present study, a putative binding site for miR-32-5p and FOXN2 was identified using the Starbase software prediction, and this interaction was experimentally validated using DLR assay. The negatively regulatory effect of miR-32-5p on FOXN2 expression was further demonstrated. Over the past decade, the PI3K/AKT pathway has garnered attention as it serves a pivotal role in orchestrating an array of cellular functions, encompassing transcription, metabolism, growth and apoptosis (42). Recently, the oncogene role of the PI3K/AKT pathway in UCEC has been elucidated, underscoring its potential as a promising therapeutic target (43,44). A PI3K/AKT inhibitor, PF-04691502, has proven to be beneficial for patients with recurrent UCEC from a clinical perspective (29). It was thus considered that a potential interaction may exist between miR-32-5p and the PI3K/AKT pathway in UCEC cells. The upregulation of miR-32-5p was found to effectively activate the PI3K/AKT pathway. Conversely, downregulation of miR-32-5p exhibited a suppressive effect on the activity of the PI3K/AKT pathway. Additionally, AKT exerts a negative regulatory effect on the function or expression of Bcl-2 homology domain 3-only proteins, which are recognized for their role in promoting cell death by deactivating the anti-cell death members of the Bcl-2 family (30). Therefore, inhibiting the PI3K/AKT signaling pathway has been demonstrated to promote apoptosis in UCEC cells (30). The present study further demonstrated that the upregulation of miR-32-5p could effectively increase the expression levels of Bcl-2, whereas its downregulation exerted inhibitory effects on Bcl-2 expression. Collectively, the present findings suggested that miR-32-5p may exert its regulatory effects on UCEC by targeting the FOXN2/PI3K/AKT/Bcl-2 pathway, thereby promoting proliferation and migration while inhibiting apoptosis.

The increasing attention towards miRNAs in exosomes stems from their pivotal role in recruiting and reprogramming essential components of the tumor microenvironment (45,46). miRNAs in exosomes are also considered vital for inter-cellular communication through cell-to-cell contact (47). Numerous reports have demonstrated that the transfer of miRNA through exosomes alters the microenvironment of tumors, ultimately contributing to the tumorigenesis of UCEC. For example, Yao *et al* (48) identified four hub exosomal miRNAs including miR-320d, miR-193a-5p, miR-99b-3p and miR-17-3p based on bioinformatic analysis, and demonstrated their potential as prognostic biomarkers or therapeutic targets in UCEC. Jing *et al* (16) reported that exosomal

miR-499a-5p interacts with VAV3 to suppress the growth of UCEC. Li *et al* (49) found an exosomal miR-148b from cancer-associated fibroblasts serve as a tumor suppressor in UCEC through the targeting of DNA methyltransferase 1. In the present study, considering the effects of miR-32-5p on the malignant behaviors of UCEC cells, it was further considered that exosomal miR-32-5p might induce comparable impacts on the growth, metastasis and apoptosis of UCEC cells. A co-culture system was established in the present study; Exo-miR-32-5p-inhibitor or Exo-miR-32-5p-inhibitor-NC was internalized by HEC-1-A cells, while Exo-miR-32-5p-mimic or Exo-miR-32-5p-mimic-NC was internalized by Ishikawa cells. Following internalization, Exo-miR-32-5p-inhibitor significantly suppressed the proliferative and migratory capacities, and induced apoptosis of HEC-1-A cells, while the opposite results were observed in Ishikawa cells with the Exo-miR-32-5p-mimic. These findings demonstrated the regulatory role of exosomal miR-32-5p in the malignant behaviors of UCEC cells. Furthermore, in HEC-1-A cells, the Exo-miR-32-5p-inhibitor inhibited PI3K/AKT/Bcl-2 pathway and elevated FOXN2 expression levels, whereas Exo-miR-32-5p-mimic exerted the opposite regulatory effects in Ishikawa cells. These results demonstrated that the transfer of exosomal miR-32-5p serves a pivotal role in modulating the expression levels of multiple target genes within recipient cells, which was in line with findings of previous studies (13,14). Therefore, it was demonstrated that exosomal-miR-32-5p regulates the proliferation, migration and apoptosis of UCEC through FOXN2/PI3K/AKT/Bcl-2 pathway.

There were some limitations to the present study. First, polydispersity index (PDI) serves as an important indicator that characterizes the uniformity of particle size distribution in samples. It is commonly used to evaluate the particle size distribution of exosomes (50). In this study, the absence of PDI may not accurately evaluate the purity of exosomes, thereby affecting the accuracy of experimental results. Furthermore, exosomes may exhibit agglomeration phenomenon in the samples, and PDI is an important indicator for determining agglomeration (50). If this indicator is ignored, it may not be possible to detect and handle the agglomeration issues in a timely manner, which could affect the separation and purification efficiency of exosomes (50). Therefore, when investigating exosomes in future research, PDI will be incorporated as a significant parameter to facilitate a more comprehensive identification of the extracted exosomes. Second, the sample size of patients was relatively small. Larger sample sizes should be considered in future studies. Third, cell line studies possess limitations in predicting clinical outcomes; the present study only conducted preliminary research on the regulatory mechanisms of exosomal-miR-32-5p in UCEC at the cellular level, and lacked validation of biological integrity, experimentation in an *in vivo* microenvironment and feasibility of clinical transformation, therefore further investigation in animal models is warranted.

In summary, the present study demonstrates a novel insight into the role of exosomal miR-32-5p in promoting the proliferation and migration, while inhibiting the apoptosis rate of UCEC cells through regulation of the FOXN2/PI3K/AKT/Bcl-2 pathway. The findings presented may provide information and insights for potential clinical therapeutic strategies for patients with UCEC.

Acknowledgements

Not applicable.

Funding

The present work was supported by Mechanism Study of Recombinant Human Interleukin-11 Combined with Dendritic Cell Vaccine Loading of Tumor Stem Cell Antigen in the Treatment of Head and Neck Squamous Cell Cancer (grant. no. KYC0000000807) and Mechanism study of circular RNA hsa_circ_0000523 as a competitive endogenous RNA upregulating METTL3 to promote invasion and metastasis of colon cancer (grant. no. 2024HX0021).

Availability of data and materials

The data analyzed during the current study are available from the corresponding author on reasonable request.

Authors' contributions

XinC made substantial contributions to the conception and design of the study. XinC, HL, XiaC, YC and GG made substantial contributions to the acquisition, analysis and interpretation of the data. XinC and HL drafted the manuscript. All authors critically revised the manuscript for intellectual content. XiaC, YC and GG confirmed the authenticity of all the raw data. All authors have read and approved the final manuscript.

Ethics approval and consent to participate

The present study adheres to the principles outlined in the Declaration of Helsinki, and ethical approvals have been obtained from Renmin Hospital of Wuhan University Ethics Committee (approval no. WDRY2023-K161; Wuhan, China). All participants provided informed consent.

Patient consent for publication

Not applicable.

Competing interests

The authors declare that they have no competing interests.

References

- Crosbie EJ, Kitson SJ, McAlpine JN, Mukhopadhyay A, Powell ME and Singh N: Endometrial cancer. *Lancet* 399: 1412-1428, 2022.
- Hafizz AMHA, Zin RRM, Aziz NHA, Kampan NC and Shafiee MN: Beyond lipid-lowering: Role of statins in endometrial cancer. *Mol Biol Rep* 47: 8199-8207, 2020.
- Li Y, Huang C, Kavlashvili T, Fronk A, Zhang Y, Wei Y, Dai D, Devor EJ, Meng X, Thiel KW, *et al*: Loss of progesterone receptor through epigenetic regulation is associated with poor prognosis in solid tumors. *Am J Cancer Res* 10: 1827-1843, 2020.
- Francis SR, Ager BJ, Do OA, Huang YJ, Soisson AP, Dodson MK, Werner TL, Sause WT, Grant JD and Gaffney DK: Recurrent early stage endometrial cancer: Patterns of recurrence and results of salvage therapy. *Gynecol Oncol* 154: 38-44, 2019.
- Bregar AJ, Melamed A, Diver E, Clemmer JT, Uppal S, Schorge JO, Rice LW, Del Carmen MG and Rauh-Hain JA: Minimally invasive staging surgery in women with early-stage endometrial cancer: Analysis of the national cancer data base. *Ann Surg Oncol* 24: 1677-1687, 2017.
- Connor EV and Rose PG: Management strategies for recurrent endometrial cancer. *Expert Rev Anticancer Ther* 18: 873-885, 2018.
- Pölcher M, Rottmann M, Brugger S, Mahner S, Dannecker C, Kiechle M, Brambs C, Grab D, Anthuber C, von Koch F, *et al*: Lymph node dissection in endometrial cancer and clinical outcome: A population-based study in 5546 patients. *Gynecol Oncol* 154: 65-71, 2019.
- Wessler S, Aberger F and Hartmann TN: The sound of tumor cell-microenvironment communication-composed by the cancer cluster salzburg research network. *Cell Commun Signal* 15: 20, 2017.
- Lauko A, Mu Z, Gutmann DH, Naik UP and Lathia JD: Junctional adhesion molecules in cancer: A paradigm for the diverse functions of cell-cell interactions in tumor progression. *Cancer Res* 80: 4878-4885, 2020.
- Paskeh MDA, Entezari M, Mirzaei S, Zabolian A, Saleki H, Naghdi MJ, Sabet S, Khoshbakht MA, Hashemi M, Hushmandi K, *et al*: Emerging role of exosomes in cancer progression and tumor microenvironment remodeling. *J Hematol Oncol* 15: 83, 2022.
- Wei H, Chen Q, Lin L, Sha C, Li T, Liu Y, Yin X, Xu Y, Chen L, Gao W, *et al*: Regulation of exosome production and cargo sorting. *Int J Biol Sci* 17: 163-177, 2021.
- Cully M: Exosome-based candidates move into the clinic. *Nat Rev Drug Discov* 20: 6-7, 2021.
- Au Yeung CL, Co NN, Tsuruga T, Yeung TL, Kwan SY, Leung CS, Li Y, Lu ES, Kwan K, Wong KK, *et al*: Exosomal transfer of stroma-derived miR21 confers paclitaxel resistance in ovarian cancer cells through targeting APAF1. *Nat Commun* 7: 11150, 2016.
- Baroni S, Romero-Cordoba S, Plantamura I, Dugo M, D'Ippolito E, Cataldo A, Cosentino G, Angeloni V, Rossini A, Daidone MG and Iorio MV: Exosome-mediated delivery of miR-9 induces cancer-associated fibroblast-like properties in human breast fibroblasts. *Cell Death Dis* 7: e2312, 2016.
- Che X, Jian F, Chen C, Liu C, Liu G and Feng W: PCOS serum-derived exosomal miR-27a-5p stimulates endometrial cancer cells migration and invasion. *J Mol Endocrinol* 64: 1-12, 2020.
- Jing L, Hua X, Yuanna D, Rukun Z and Junjun M: Exosomal miR-499a-5p inhibits endometrial cancer growth and metastasis via targeting VAV3. *Cancer Manag Res* 12: 13541-13552, 2020.
- Gao ZQ, Wang JF, Chen DH, Ma XS, Wu Y, Tang Z and Dang XW: Long non-coding RNA GAS5 suppresses pancreatic cancer metastasis through modulating miR-32-5p/PTEN axis. *Cell Biosci* 7: 66, 2017.
- Liang H, Tang Y, Zhang H and Zhang C: MiR-32-5p regulates radiosensitization, migration and invasion of colorectal cancer cells by targeting TOB1 gene. *Onco Targets Ther* 12: 9651-9661, 2019.
- Jin Y and Wang H: Circ_0078607 inhibits the progression of ovarian cancer via regulating the miR-32-5p/SIK1 network. *J Ovarian Res* 15: 3, 2022.
- Zhang P, Liang T, Chen Y, Wang X, Wu T, Xie Z, Luo J, Yu Y and Yu H: Circulating exosomal miRNAs as Novel biomarkers for stable coronary artery disease. *Biomed Res Int* 2020: 3593962, 2020.
- Zhou L, Wang W, Wang F, Yang S, Hu J, Lu B, Pan Z, Ma Y, Zheng M, Zhou L, *et al*: Plasma-derived exosomal miR-15a-5p as a promising diagnostic biomarker for early detection of endometrial carcinoma. *Mol Cancer* 20: 57, 2021.
- Berek JS, Matias-Guiu X, Creutzberg C, Fotopoulou C, Gaffney D, Kehoe S, Lindemann K, Mutch D and Concin N; Endometrial Cancer Staging Subcommittee, FIGO Women's Cancer Committee: FIGO staging of endometrial cancer: 2023. *Int J Gynaecol Obstet* 162: 383-394, 2023.
- Pan Y, Wang X, Li Y, Yan PY and Zhang H: Human umbilical cord blood mesenchymal stem cells-derived exosomal microRNA-503-3p inhibits progression of human endometrial cancer cells through downregulating MEST. *Cancer Gene Ther* 29: 1130-1139, 2022.
- Livak KJ and Schmittgen TD: Analysis of relative gene expression data using real-time quantitative PCR and the 2(-Delta Delta C(T)) method. *Methods* 25: 402-408, 2001.

25. Zhu Z, Chen Z, Wang M, Zhang M, Chen Y, Yang X, Zhou C, Liu Y, Hong L and Zhang L: Detection of plasma exosomal miRNA-205 as a biomarker for early diagnosis and an adjuvant indicator of ovarian cancer staging. *J Ovarian Res* 15: 27, 2022.
26. Liu W, Yang D, Chen L, Liu Q, Wang W, Yang Z, Shang A, Quan W and Li D: Plasma exosomal miRNA-139-3p is a novel biomarker of colorectal cancer. *J Cancer* 11: 4899-4906, 2020.
27. Taghehchian N, Lotfi M, Zangouei AS, Akhlaghpour I and Moghbeli M: MicroRNAs as the critical regulators of Forkhead box protein family during gynecological and breast tumor progression and metastasis. *Eur J Med Res* 28: 330, 2023.
28. Xie SM, Zhang Q and Jiang L: Current knowledge on exosome biogenesis, cargo-sorting mechanism and therapeutic implications. *Membranes (Basel)* 12: 498, 2022.
29. Jiang N, Dai Q, Su X, Fu J, Feng X and Peng J: Role of PI3K/AKT pathway in cancer: The framework of malignant behavior. *Mol Biol Rep* 47: 4587-4629, 2020.
30. He Y, Sun MM, Zhang GG, Yang J, Chen KS, Xu WW and Li B: Targeting PI3K/Akt signal transduction for cancer therapy. *Signal Transduct Target Ther* 6: 425, 2021.
31. Pavlidou A and Vlahos NF: Molecular alterations of PI3K/Akt/mTOR pathway: A therapeutic target in endometrial cancer. *ScientificWorldJournal* 2014: 709736, 2014.
32. Buhtoiarova TN, Brenner CA and Singh M: Endometrial carcinoma: Role of current and emerging biomarkers in resolving persistent clinical dilemmas. *Am J Clin Pathol* 145: 8-21, 2016.
33. Hu ZY, Tang LD, Zhou Q, Xiao L and Cao Y: Aberrant promoter hypermethylation of p16 gene in endometrial carcinoma. *Tumour Biol* 36: 1487-1491, 2015.
34. Muinelo-Romay L, Casas-Arozamena C and Abal M: Liquid biopsy in endometrial cancer: New opportunities for personalized oncology. *Int J Mol Sci* 19: 2311, 2018.
35. Falcone G, Felsani A and D'Agnano I: Signaling by exosomal microRNAs in cancer. *J Exp Clin Cancer Res* 34: 32, 2015.
36. Bjørnestrø T, Redalen KR, Meltzer S, Thusyanthan NS, Samiappan R, Jegerschöld C, Handeland KR and Ree AH: An experimental strategy unveiling exosomal microRNAs 486-5p, 181a-5p and 30d-5p from hypoxic tumour cells as circulating indicators of high-risk rectal cancer. *J Extracell Vesicles* 8: 1567219, 2019.
37. Zheng M, Hou L, Ma Y, Zhou L, Wang F, Cheng B, Wang W, Lu B, Liu P, Lu W and Lu Y: Exosomal let-7d-3p and miR-30d-5p as diagnostic biomarkers for non-invasive screening of cervical cancer and its precursors. *Mol Cancer* 18: 76, 2019.
38. Panda AC: Circular RNAs Act as miRNA sponges. *Adv Exp Med Biol* 1087: 67-79, 2018.
39. Zeng ZL, Zhu Q, Zhao Z, Zu X and Liu J: Magic and mystery of microRNA-32. *J Cell Mol Med* 25: 8588-8601, 2021.
40. Liu YJ, Zhou HG, Chen LH, Qu DC, Wang CJ, Xia ZY and Zheng JH: MiR-32-5p regulates the proliferation and metastasis of cervical cancer cells by targeting HOXB8. *Eur Rev Med Pharmacol Sci* 23: 87-95, 2019.
41. Wang R, Huang Z, Qian C, Wang M, Zheng Y, Jiang R and Yu C: LncRNA WEE2-AS1 promotes proliferation and inhibits apoptosis in triple negative breast cancer cells via regulating miR-32-5p/TOB1 axis. *Biochem Biophys Res Commun* 526: 1005-1012, 2020.
42. Lawrence MS, Stojanov P, Mermel CH, Robinson JT, Garraway LA, Golub TR, Meyerson M, Gabriel SB, Lander ES and Getz G: Discovery and saturation analysis of cancer genes across 21 tumour types. *Nature* 505: 495-501, 2014.
43. Wei ST, Zhang J, Zhao R, Shi R, An L, Yu Z, Zhang Q, Zhang J, Yao Y, Li H and Wang H: Histone lactylation promotes malignant progression by facilitating USP39 expression to target PI3K/AKT/HIF-1 α signal pathway in endometrial carcinoma. *Cell Death Discov* 10: 121, 2024.
44. Ma LJ, Huang WN, Liang XL, Bai G, Wang X, Jiang H, Xin Y, Hu L, Chen X and Liu C: Inhibition of squalene epoxidase linking with PI3K/AKT signaling pathway suppresses endometrial cancer. *Cancer Sci* 114: 3595-3607, 2023.
45. Li C, Zhou T, Chen J, Li R, Chen H, Luo S, Chen D, Cai C and Li W: The role of exosomal miRNAs in cancer. *J Transl Med* 20: 6, 2022.
46. Nail HM, Chiu CC, Leung CH, Ahmed MMM and Wang HMD: Exosomal miRNA-mediated intercellular communications and immunomodulatory effects in tumor microenvironments. *J Biomed Sci* 30: 69, 2023.
47. Fasken MB, Morton DJ, Kuiper EG, Jones SK, Leung SW and Corbett AH: The RNA exosome and human disease. *Methods Mol Biol* 2062: 3-33, 2020.
48. Yao Y, Shi L and Zhu X: Four differentially expressed exosomal miRNAs as prognostic biomarkers and therapy targets in endometrial cancer: Bioinformatic analysis. *Medicine (Baltimore)* 102: e34998, 2023.
49. Li BL, Lu W, Qu JJ, Ye L, Du GQ and Wan XP: Loss of exosomal miR-148b from cancer-associated fibroblasts promotes endometrial cancer cell invasion and cancer metastasis. *J Cell Physiol* 234: 2943-2953, 2019.
50. Wang Y, Guo MM, Lin DM, Liang D, Zhao L, Zhao R and Wang Y: Docetaxel-loaded exosomes for targeting non-small cell lung cancer: preparation and evaluation in vitro and in vivo. *Drug Deliv* 28: 1510-1523, 2021.



Copyright © 2026 Chen et al. This work is licensed under a Creative Commons Attribution-NonCommercial-NoDerivatives 4.0 International (CC BY-NC-ND 4.0) License.